UNIVERSITÄT AUGSBURG
Universitätsbibliothek

OPEN ACCESS
OPUS AUGSBURG

# AAV-mediated expression of AP-1-neutralizing RNA decoy oligonucleotides attenuates transplant vasculopathy in mouse aortic allografts

**Anca Remes, Maximilian Franz, Franziska Mohr, Antje Weber, Kleopatra Rapti, Andreas Jungmann, Matthias Krack, Markus Hecker, Klaus Kallenbach, Oliver J. Müller, Rawa Arif, Andreas H. Wagner**

**Angaben zur Veröffentlichung / Publication details:**

Remes, Anca, Maximilian Franz, Franziska Mohr, Antje Weber, Kleopatra Rapti, Andreas Jungmann, Matthias Krack, et al. 2019. "AAV-mediated expression of AP-1-neutralizing RNA decoy oligonucleotides attenuates transplant vasculopathy in mouse aortic allografts." *Molecular Therapy –Methods & Clinical Development* 15: 246–56.
https://doi.org/10.1016/j.omtm.2019.09.009.

**Nutzungsbedingungen / Terms of use:**

**CC BY-NC-ND 4.0**

*Dieses Dokument wird unter folgenden Bedingungen zur Verfügung gestellt: / This document is made available under these conditions:*
***CC-BY-NC-ND 4.0: Creative Commons: Namensnennung - Nicht kommerziell - Keine Bearbeitung***
*Weitere Informationen finden Sie unter: / For more information see:*
*https://creativecommons.org/licenses/by-nc-nd/4.0/deed.de*

Molecular Therapy
Methods & Clinical Development
Original Article

# AAV-Mediated Expression of AP-1-Neutralizing RNA Decoy Oligonucleotides Attenuates Transplant Vasculopathy in Mouse Aortic Allografts

Anca Remes,[1,7] Maximilian Franz,[2,7] Franziska Mohr,[3] Antje Weber,[2] Kleopatra Rapti,[4] Andreas Jungmann,[5] Matthias Karck,[2] Markus Hecker,[3] Klaus Kallenbach,[6] Oliver J. Müller,[1] Rawa Arif,[2,7] and Andreas H. Wagner[3,7]

[1]Department of Internal Medicine III, University of Kiel and University Hospital Schleswig-Holstein, Kiel, and German Centre for Cardiovascular Research, Partner Site Hamburg/Kiel/Lübeck, Germany; [2]Department of Cardiac Surgery, University Hospital Heidelberg, 69120 Heidelberg, Germany; [3]Institute of Physiology and Pathophysiology, Heidelberg University, 69120 Heidelberg, Germany; [4]BioQuant Center, Heidelberg University, 69120 Heidelberg, Germany; [5]Internal Medicine III, University Hospital Heidelberg, 69120 Heidelberg, Germany; [6]Department of Cardiac Surgery, INCCI HaerzZenter, 1210 Luxembourg, Luxembourg

**Transplant vasculopathy (TV), characterized by obstructive lesions in affected vessels, represents one of the long-term complications of cardiac transplantation. Activation of the transcription factor activator protein-1 (AP-1) is implicated in smooth muscle cell (SMC) phenotypic switch from contractile to synthetic function, increasing the migration and proliferation rate of these cells. We hypothesize that adeno-associated virus (AAV)-mediated delivery of an RNA hairpin AP-1 decoy oligonucleotide (dON) might effectively ameliorate TV severity in a mouse aortic allograft model. Aortic allografts from DBA/2 mice *ex vivo* transduced with modified AAV9-SLR carrying a targeting peptide within the capsid surface were transplanted into the infrarenal aorta of C57BL/6 mice. Cyclosporine A (10 mg/kg BW) was administered daily. AP-1 dONs were intracellularly expressed in the graft tissue as small hairpin RNA proved by fluorescent *in situ* hybridization. Explantation after 30 days and histomorphometric evaluation revealed that AP-1 dON treatment significantly reduced intima-to-media ratio by 41.5% ($p < 0.05$) in the grafts. In addition, expression of adhesion molecules, cytokines, as well as numbers of proliferative SMCs, matrix metalloproteinase-9-positive cells, and inflammatory cell infiltration were significantly decreased in treated aortic grafts. Our findings demonstrate the feasibility, efficacy, and specificity of the anti-AP-1 RNA dON approach for the treatment of allograft vasculopathy in an animal model. Moreover, the AAV-based approach in general provides the possibility to achieve a prolonged delivery of nucleic-acids-based therapeutics in to the blood vessel wall.**

## INTRODUCTION

Transplant vasculopathy (TV) remains one of the main complications hindering long-term graft survival, thus representing a major risk factor for mortality in patients subjected to solid organ transplantation. Although acute cellular rejection can be controlled with immunosuppressive drugs such as cyclosporine A (CsA) or tacrolimus, grafts with significant initimal thickening and accelerated progression of cardiac allograft vasculopathy CAV have the poorest survival prognosis.[1]

On the cellular level, intense proliferation and migration of activated smooth muscle cells (SMC) initiates intimal lesion formation that can lead to graft failure.[2,3] Additionally, an imbalance between extracellular matrix degradation and deposition contributes to intense remodeling associated with TV. These pathological events lead to blood vessel obstruction and eventually to transplanted graft failure.[4]

Activator protein-1 (AP-1) is one of the main transcription factors involved in SMC proliferation and functional modulation from a contractile to a synthetic phenotype.[5] AP-1 family members induce cell growth and matrix metalloprotease expression in response to inflammatory cytokines and oxidative stress.[6–9] Additionally, AP-1 is critically involved in transcriptional modulation of inflammatory cytokines.[10–12] Therefore, neutralization of AP-1-dependent signaling pathways may potentially be translated into a promising therapeutic strategy for TV. Indeed, local AP-1 decoy oligodeoxynucleotide (dODN) application decreased the severity of neointimal lesions in coronary arteries of hypercholesterolemic minipigs after percutaneous transluminal coronary angioplasty.[13] Furthermore, *ex vivo* perfusion with AP-1 and signal transducer and activator of transcription-1 (STAT-1) decoy ODNs prevented acute rejection and prolonged cardiac graft survival in rat heart allografts.[14,15]

Here, we describe a long-term strategy to inhibit AP-1 transcriptional activity by intracellular expression of neutralizing RNA decoy oligonucleotides (dONs) accomplished through adeno-associated virus (AAV) vectors and its preclinical validation in a mouse TV model. As heterotopic aortic transplantation leads to early graft occlusion and consecutive death of the recipients within the first 10 postoperative days

Received 30 April 2019; accepted 24 September 2019;
https://doi.org/10.1016/j.omtm.2019.09.009.

[7]These authors contributed equally to this work.

**Correspondence:** Andreas H. Wagner, PhD, Institute of Physiology and Pathophysiology, Heidelberg University, Im Neuenheimer Feld 326, 69120 Heidelberg, Germany.
**E-mail:** a.wagner@physiologie.uni-heidelberg.de


This is an open access article under the CC BY-NC-ND license (http://creativecommons.org/licenses/by-nc-nd/4.0/).

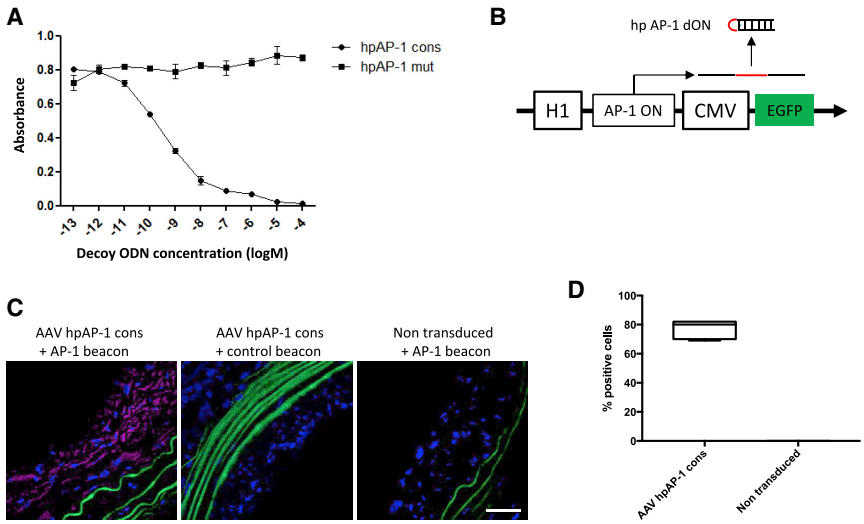



**Figure 1. hpAP-1 dODN Specificity and Generation in Aortic Grafts following Transduction**

(A) Transcription factor ELISA proving *in situ* the specificity of the designed sequence in binding to the transcription factor. (B) Schematic presentation of hairpin (hp) AP-1 dON generation following transduction. The H1 promoter drives the single-stranded RNA hpAP-1 dODN expression, which spontaneously base pairs to form hairpin (red, loop sequence). CMV promoter drives EGFP expression as positive control for transduction. (C) Representative images of fluorescence *in situ* hybridization experiments showing the presence of hpAP-1 dONs in transduced aortic tissue 30 days after initial surgery. A molecular beacon with red fluorescence (Cy5) was used to detect specifically dONs; nuclei were stained with DAPI (blue). Elastin autofluorescence was recorded on the green channel. Scale bar represents 25 μm (n = 9). (D) AAV9SLR transduction efficacy. Nuclei were marked using DAPI in order to count the number of cells/field of view. Four representative fields per section and two sections per graft were examined (n = 9).

without immunosuppressive therapy,[16] we used CsA in our study. Short-term *ex vivo* incubation with the AAV vector solution allows transduction and continuous long-term expression of the active nucleic acid drug as small hairpin RNA (shRNA) in vascular target cells and exerts a profound therapeutic effect by alleviating lumen stenosis.

## RESULTS

### hpAP-1 dODN Specificity and Binding Affinity

The apparent affinity with which the hairpin AP-1 (hpAP-1) dODN specifically binds to the target transcription factor was determined by an ELISA approach. In this assay, a nuclear extract from stimulated cells containing the activated AP-1 transcription factor is allowed to bind to an immobilized double-stranded DNA (dsDNA) probe comprising its consensus sequence. The binding and the displacement of AP-1 from this probe by the hpAP-1 dODN was visualized by using a specific antibody against the active form of AP-1 (Figure 1). The average apparent affinity expressed as half maximal inhibitory concentration ($IC_{50}$) was determined at 2.5 nM for the consensus hpODN. The corresponding mutated control hpODN does not seem to bind to the transcription factor in the tested range of concentrations.

### Tissue-Specific hpAP-1 Decoy ON Expression after AAV Serotype 9 (AAV9)SLR Transduction

Next, we confirmed the expression and presence of hpAP-1 RNA dONs in aortic tissue transduced with the designed vector (Figure 1B) 30 days after transplantation. For this purpose, 7-μm-thick aortic frozen sections were subjected to fluorescence *in situ* hybridization (FISH) analysis (n = 9 animals, 2 sections/mouse). As shown in Figures 1C and 1D, 80% ± 2% of neointimal cells expressed hpAP-1 decoy ODNs, proving successful transduction and generation of the active nucleic acid drug 30 days after *ex vivo* transduction and reimplantation into recipient mice. No fluorescent signal was detected in non-transduced tissue or in samples using a non-related control molecular beacon, demonstrating the specificity of the detection method.

### AAV9SLR-Mediated hpAP-1 dON Delivery Attenuates Neointima Formation

Morphometric analysis revealed that control non-treated mice developed vascular lesions and intense remodeling, accompanied by high degrees of vessel lumen obstruction. In these grafts, an increased expression of the AP-1 family member c-Jun and also c-Jun N-terminal kinase (JNK) could be demonstrated (Figure S1). Similarly, treatment with AAV9SLR expressing the mutated control hpAP-1 dONs had no effect on this parameter, whereas the consensus hpAP-1 dON delivery led to a significant decrease in neointima formation, proven by a neointima/media ratio reduction of 41.5% compared to controls (Figure 2).

### AAV9SLR-Mediated hpAP-1 dON Delivery Decreases SMC Proliferation

SMC proliferation has been shown to be an initial event in response to vascular injury, contributing to neointima formation in various animal models of TV.[17] Elucidating the molecular mechanisms of the observed therapeutic effects, we analyzed cyclin D2 expression as a regulatory protein of the cell cycle[18] in the transplanted aortic tissue. Compared to control groups, grafts transduced with AAV9SLR expressing hpAP-1 consensus dONs exhibited a significant 2.6-fold decline ($p < 0.05$) and 3-fold ($p < 0.01$) decline in cyclin D2-positive SMC population in the neointima compared to control and mutated AAV, respectively (Figure 3).

### AAV9SLR-Mediated hpAP-1 dON Delivery Mitigates Immune Cell Infiltration

Immune cell infiltration into the aortic tissue is a well-characterized process that contributes to graft rejection.[19–21] Recruitment of inflammatory cells involves the expression of adhesion molecules such as, e.g., VCAM-1.[19,22] As previously reported,[23,24] we detected

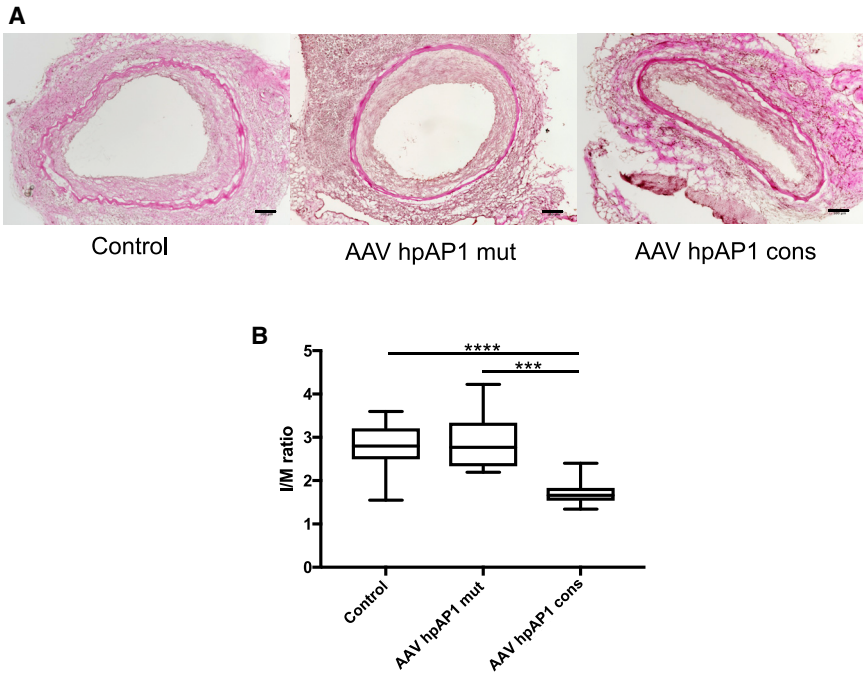



**Figure 2. Prevention of Neointima Formation following AAV9SLR-Mediated Delivery of hpAP-1 cons dONs**

(A) Representative images of H&E stainings of transplanted aortic grafts that received the mentioned treatments, 30 days after surgery. (B) Box-and-whisker plot of neointima/media ratios, as a measure of lumen obstruction. Horizontal bars in the boxes indicate median values, boxes indicate interquartile range, and whiskers indicate range of non-outlier values. Scale bar represents 100 μm (***$p < 0.01$, ****$p < 0.0001$; n = 14 for control, n = 7 for AAV hpAP-1 mut, n = 9 for AAV hpAP-1 cons).

VCAM-1 expression not only in endothelial cells but also in neointimal SMCs in control groups, while it was significantly decreased by 70% and 64.9% ($p < 0.05$) in aortic tissue receiving gene therapy, as compared to control and AAV hpAP-1 mut-treated grafts, respectively (Figure 4). Furthermore, we analyzed the degree of macrophage and $CD4^+$ T cell accumulation in aortic grafts of the different treatment groups. As expected, we detected highly abundant inflammatory cell infiltrates in control tissue in both neointima and media (Figure 5). Inhibition of AP-1 target genes like leukocyte adhesion molecule VCAM-1 led to a significant 3-fold ($p < 0.05$) reduction in CD4-positive T-lymphocyte infiltration related to control and 2.6-fold ($p < 0.01$) compared to mutated AAV (Figures 5A and 5B). Moreover, we found a 50% decrease in monocyte/macrophage accumulation as compared to control non-treated grafts and 52% related to AAV hpAP-1 mut-transduced tissue ($p < 0.05$) (Figures 5C and 5D).

### AAV9SLR-Mediated hpAP-1 dON Delivery Attenuates Pro-inflammatory Cytokine Expression in Transduced Aortic Allografts

The observed reduction of monocyte infiltration in the aortic tissue has led to the assumption that pro-inflammatory and chemotactic cytokines are decreased following AP-1 neutralization in transduced aortic grafts. Indeed, interleukin-6 (IL-6), interferon-γ (IFN-γ), and monocyte chemotactic protein-1 (MCP-1) mRNA expression was significantly reduced in AAV9SLR hpAP-1 cons-treated grafts, whereas the control treatment had no effect (Figures 6A–6C). Analyses of frozen graft sections confirmed a significant decrease in IL-6 (43% compared to control, 40% related to AAV hpAP-1 mut) and MCP-1 (59% compared to control and 54 related to AAV hpAP-1 mut) expression on the protein level (Figures 6D–6G).

### AAV9SLR-Mediated hpAP-1 dON Delivery Does Not Decrease MMP2 Protein Level but Reduces the Amount of Infiltrating MMP9-Positive Cells

Taking into account the major role of matrix metalloproteinases in development and progression of TV,[3] we next studied whether our treatment affected MMP2 and MMP9 protein expression in aortic sections. Thirty days after surgery, we could not detect any significant difference in MMP2 expression levels between the different treatment groups (Figures 7A and 7B). In contrast to MMP2-positive cells located mostly in the media or myointimal cells, MMP9 protein predominantly was found in the adventitia. Additionally, MMP2 was more widely expressed than MMP9 in the graft tissue. We next analyzed the density of MMP9-positive cells (number of cells/tissue area) and compared this parameter between the treatment groups. hpAP-1 dON treatment led to a significant decrease in the numbers of MMP9-positive cells as compared to aortic tissue, which received control treatment (Figures 7C and 7D). Interestingly, we observed single MMP9-positive cells in the neointimal area of control grafts, which cannot be detected in AAV hpAP1cons-treated grafts. To characterize these observed infiltrating cells, we performed co-staining with established markers of macrophages (F4/80), immune cells (CD54ICAM-1), activated fibrogenic cells/myofibroblasts (α-SMA), and progenitor cells (Sca-1). We could identify a small subset of MMP9-expressing cells as an intercellular adhesion molecule-1 (ICAM-1)-positive immune cell population, while most of the MMP9-immunopositive cells were of different origin (Figure 7E).

## DISCUSSION

Heart transplantation remains the treatment of choice for patients suffering from end-stage heart failure.[25] The high risk of TV development is a determinant factor of graft and patient survival.[26] Long-term administration of immunosuppressive drugs for the management of autoimmune inflammatory conditions has been proven to be successful in decreasing the rate of chronic organ rejection. However, this treatment is associated with notable side effects like elevated risk for infection, malignancy, cardiovascular disease, and bone marrow suppression.[27] In our study, the main rationale of the CsA immunosuppressive strategy was the necessity for the feasibility of

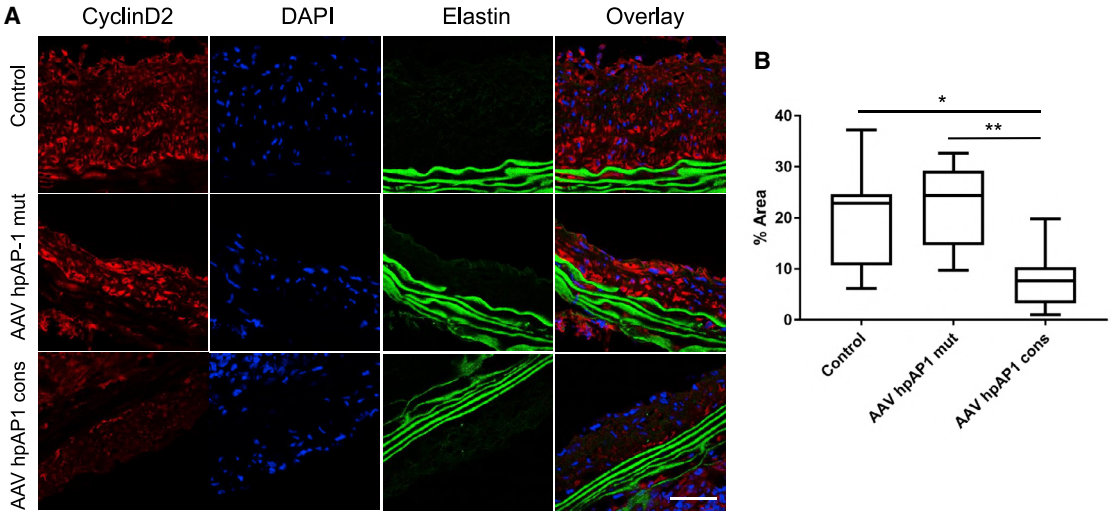



**Figure 3. Decreased Cell Proliferation following AAV9SLR-Mediated Delivery of hpAP-1 cons dONs**

(A) Representative images showing immunohistochemical staining against cyclin D2 (red) as a marker of proliferating cells. DAPI (blue) was used to mark cell nuclei, and elastin autofluorescence was recorded on the green channel. (B) Box-and-whisker plot of the level of proliferating cells, measured as percentage area of cyclin D2-positive cells in the neointima. Horizontal bars in the boxes indicate median values, boxes indicate interquartile range, and whiskers indicate range of non-outlier values (*$p < 0.05$, **$p < 0.01$; n = 14 for control, n = 7 for AAV hpAP-1 mut, n = 9 for AAV hpAP-1 cons).

the animal model of heterotopic transplantation model. Without immunosuppression, interposition of an aortic graft from DBA/2 mouse strain into the C57BL/6J recipient strain leads to acute cell-mediated rejection, which completely eliminates all donor-derived vascular cells from the graft within 2–3 weeks, creating a highly artifactual situation of limited relevance as a model for the changes in graft vessels that occur in the clinic.[28] AAV is a versatile viral vector technology that can be engineered for very specific functionality in gene therapy. It has the potential to overcome the side effects of immunosuppressive drugs by offering the possibility of *ex vivo* transduction of the transplant prior to implantation. AAV vectors are powerful tools for gene transfer directed into the vasculature, not only due to their low immunogenicity compared adenovirus and sustained expression of the delivered gene,[29] but also for their capacity to transduce both proliferating and non-proliferating cells.[30] To the best of our knowledge, this is the first report describing an AAV9-based therapy approach with the targeting peptide SLRSPP in a mouse model for TV. SLRSPP has been shown to increase the transduction efficiency in human coronary artery endothelial and smooth muscle cells.[31] Based on a recent study, we designed a hairpin decoy ODN utilizing the mechanism of shRNA expression.[32] Instead of working as a tool for RNAi, the shRNA bearing binding site herein neutralized efficiently AP-1 transcription factors. We can exclude the degradation of mRNA as an unspecific side effect, as the loop structure of our shRNA AP-1 decoy ODN sequence does not include the dsRNA sequence targeting RNASse III enzymes like, e.g., Drosha and Dicer, important for RNAi-dependent sequence-specific gene silencing.[33]

AP-1 transcription factor is one of the regulators of both MMPs and pro-inflammatory cytokine production and a highly promising target for inhibiting TV development. Indeed, we could demonstrate an up-regulation of endogenous AP-1 levels after transplantation, which highlights the importance of AP-1 blockage with dON. Previous studies already showed that application of dODNs modulating AP-1 transcriptional activity attenuates neointima formation by decreasing the proliferative SMC capacities and inhibits inflammatory signaling pathways.[15,34] Moreover, we have recently shown that AP-1 dODN application to tissue grafts prior to aortic transplantation can significantly reduce the development of TV in the same animal model by reducing SMC migration and decreasing the infiltration of inflammatory monocytes into the neointima.[35] Although local application of decoy ODNs has been proven effective, our approach provides the possibility to achieve a long-term formation of AP-1 decoy ONs in aortic smooth muscle cells after a single short-time incubation period.

In accordance with previous studies,[34,36] we observed that AP-1 dONs inhibited proliferation of neointimal SMCs and neointimal formation, as shown by cyclin D2-staining results. The effectiveness can be explained by functional AP-1 binding sites in the promoter of this cell-cycle regulator protein.[37] In addition, AP-1 decoy ODN has been described to significantly decrease SMC migration and arterial tissue remodeling.[38]

It has been reported that TV is a highly dynamic process, involving not only activated SMCs, but also cells resident in the adventitia and infiltrating inflammatory cells.[39] The contribution of macrophages and activated T cells is a critical factor leading to TV formation.[40] AP-1 activation creates a pro-inflammatory milieu by regulating cytokines such as MCP-1, involved in monocyte recruitment and

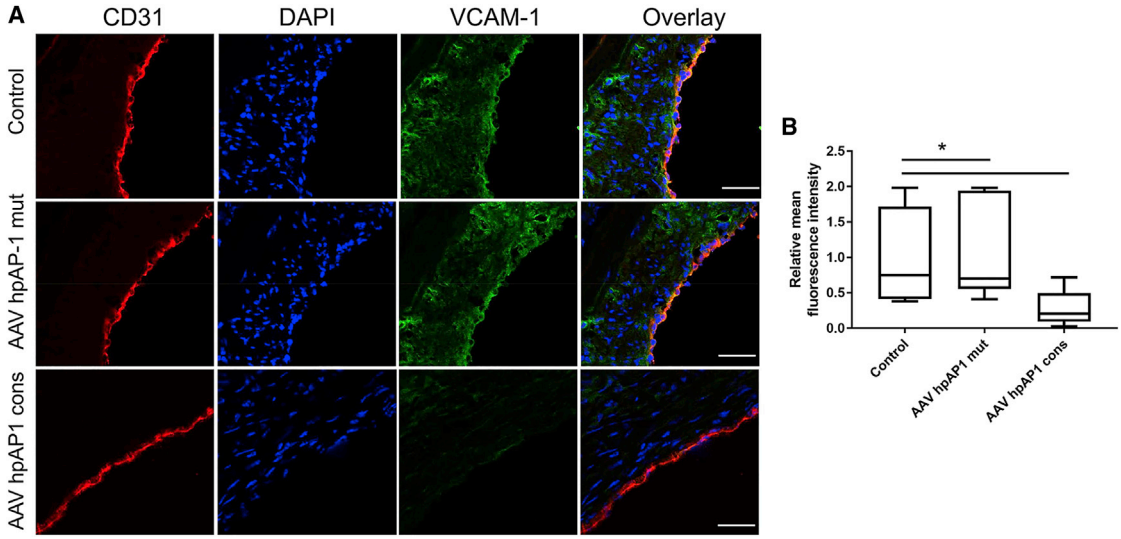



**Figure 4. Decreased VCAM-1 Protein Level following AAV9SLR-Mediated Delivery of hpAP-1 cons dONs**

(A) Representative images showing VCAM-1 (green) immunohistochemistry of grafts receiving the specified vectors. CD31 immunohistochemistry (red) was used to mark specifically endothelial cells, and DAPI (blue) labeled cell nuclei. (B) Box-and-whisker plot of mean fluorescence intensity detected in the green channel. Horizontal bars in the boxes indicate median values, boxes indicate interquartile range, and whiskers indicate range of non-outlier values (*$p < 0.05$ versus control; n = 14 for control, n = 7 for AAV hpAP-1 mut, n = 9 for AAV hpAP-1 cons). Scale bar represents 25 μm.

differentiation.[41] In turn, activated macrophages secrete pro-inflammatory cytokines such as IL-1, IL-12, tumor necrosis factor alpha (TNF-α), and IFN-γ, which further enhance SMC proliferation, migration, and lesion formation.[42] Importantly, the AP-1 transcription factor family was shown to promote the expression of the leukocyte adhesion molecule VCAM-1, essential for recruitment of monocytes and T cells and migration into arterial tissue.[43,44] Moreover, AP-1 blockade by adenovirus-mediated overexpression of a dominant-negative form of c-Jun in endothelial cells led to inhibition of ICAM-1 induction and functionally, to a decreased monocyte migration and infiltration.[45] In line with these findings, we could detect a remarkable decrease in VCAM-1 protein level in graft expression the AP1 cons dON, which correlated with a marked reduction in macrophage and T cell numbers present in the aortic wall, as well as decreased pro-inflammatory markers IL-6 and MCP-1.

MMP2 and MMP9 are crucial for the metabolism of the major basement membrane constituent collagen type IV. Like described before,[46] we found these two gelatinases differentially regulated in regard to graft remodeling. MMP2 protein abundance was higher than MMP9 in the graft tissue and mainly located throughout the myointima and media, as previously described for vein graft remodeling.[46] The hpAP-1 dON approach failed to inhibit MMP2 but not MMP9 expression, which strengthened the assumption that the two gelatinases are differentially regulated on the transcriptional level. Indeed, in rodents, the promoter region of MMP9 contains a conserved proximal AP-1 binding site, whereas that of the MMP2 has a non-canonical AP-1 binding site,[47] different from the consensus binding site present in our hpAP-1 dON. Non-canonical sequences can be recognized by various AP-1 complexes to control gene expression.[48] Therefore, is seems that AP-1 plays a critical role in MMP9 expression but simply acts as one of several other regulatory transcription factors, explaining the lack of effectivity of our dON approach in case of MMP2.

Interestingly, we identified small subset of MMP9-positive cells in the neointima of control grafts that could be positively stained for ICAM-1 but were negative for markers like F4/80 (macrophages), Sca-1 (progenitor cells), or α-SMA (activated fibrogenic cells/myofibroblasts). MMP9 is known for long time to play a key role in smooth muscle cell migration during neointima formation.[49,50] ICAM-1 on smooth muscle cells in the neointima may contribute to the inflammatory reaction in the vascular wall by playing a role for leukocyte accumulation and activation of mononuclear cells,[51] which might lead to prolongation of the inflammatory response within diseased blood vessels.[52] However, most of the other MMP9 immunopositive cells were of different origin, which will be examined in a separate study.

Despite the effectiveness of the single graft pre-treatment with AAV9SLR vector expressing hpAP-1 dON as shRNA in mice, our study has some limitations in regard to the human application. Longer experimental follow-up periods than 30 days were not tested so far. AAVs are not immunogenic in mice, but its immunogenicity becomes apparent in large-animal models and human subjects.[53] Humans are natural hosts of AAVs and exhibit a high seroprevalence against AAV vectors, which limits the widespread application of AAV vectors into patients with pre-existing neutralizing antibodies or memory T cells. Strategies to circumvent humoral immunity to adeno-associated viral vectors are currently in the development phase.[54] However, for clinical application, the AAV solution can be added to

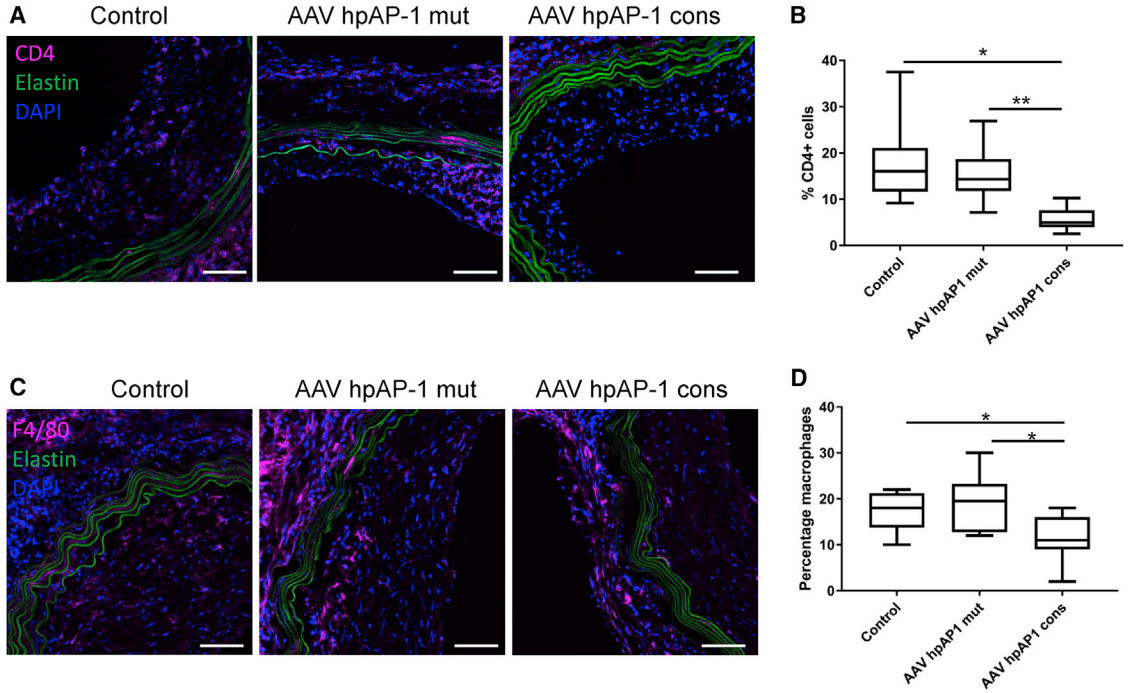



**Figure 5. Decreased Immune Cell Infiltration following AAV9SLR-Mediated Delivery of hpAP-1 cons dONs**

(A and B) Representative images (A) and box-and-whisker plot (B) showing immunohistochemical analyses of CD4-positive cells in the aortic tissues of the mentioned treatment groups (*$p < 0.05$ and **$p < 0.01$ versus control). (C and D) Representative images (C) and box-and-whisker plot (D) showing immunohistochemical analysis of F4/80-positive monocytes/macrophages in the aortic tissues of the mentioned treatment groups. DAPI (blue) marks cell nuclei, and elastin autofluorescence is shown in green. Scale bar represents 25 μm. Horizontal bars in the boxes indicate median values, boxes indicate interquartile range, and whiskers indicate range of non-outlier values (*$p < 0.05$; n = 14 for control, n = 7 for AAV hpAP-1 mut, n = 9 for AAV hpAP-1 cons).

the priming or maintenance solution of the TransMedics organ care System (OCS) heart perfusion systems. This device allows preservation of the donor heart by perfusing the organ at 34°C in a beating state, potentially reducing the detrimental effect of cold storage,[55] and can be used to transport donor hearts in this state.[56] In conclusion, our study offers a therapeutic approach centered on AAV-mediated long-term delivery of RNA hairpin dONs neutralizing AP-1 transcriptional activity, which effectively reduced vascular lesion severity.

## MATERIALS AND METHODS

### Hairpin dODN Technology, Molecular Cloning, and AAV Production

The sequences of the dODNs (Biomers, Ulm, Germany) used in our study were 5′-CTGCG*GTGCTGACTCAGCAC*GAAAC*GTGCTCAG TGAGCAC*CGCAG-3′ (hairpin AP-1 consensus decoy ODN, binding site shown in italics) and 5′-CTGCG*GTGCTTACTTAGCAC* GAAAC*GTGCTAAGTAAGCAC*CGCAG-3′ (non-functional hairpin AP-1 control dODN, mutated base pairs are underlined).

The hairpin AP-1 dODN was designed as a single-stranded homoduplex molecule consisting of a small loop and a long beacon stem that contains the transcription factor binding site. The initially single-stranded hairpin AP-1 dODN quickly hybridizes to itself representing the active double-stranded ODN subsequently modulating effective gene expression.[38,57]

The dODNs sequences were cloned intro a pDS backbone under the control of H1 promoter. In addition, the plasmid contains EGFP as an expression marker, initiated by Cytomegalovirus (CMV) promoter (Figure S2). Individual dODNs were synthesized (GeneArt, Thermo Fisher Scientific, Darmstadt, Germany) with the addition of SalI (5′) and KasI (3′) restriction sites and cloned individually into the pDS backbone. The correct decoy ODNs insertion was validated by sequencing using a forward primer binding to H1 promoter (Eurofins, Ebersberg, Germany).

AAV9 vectors[31] were generated by co-transfection of adenoviral helper plasmid pDGΔVP, the endothelial-specific AAV9 capsid variant p5E18VD2/9-SLRSPPS and either genome plasmid pDS-H1-hpAP1cons-CMV-EGFP or -hpAP1mut. AAV9SLR vectors were then purified using iodixanol step gradient ultracentrifugation as described previously.[58–60] Genomic titers were determined by quantitative real-time PCR.[58,61]

### Assessment of AP-1 dODN Specificity

A sandwich ELISA-based method was employed to test the binding affinity of the hpAP-1 dODNs (Active Motif, Carlsbad, CA,

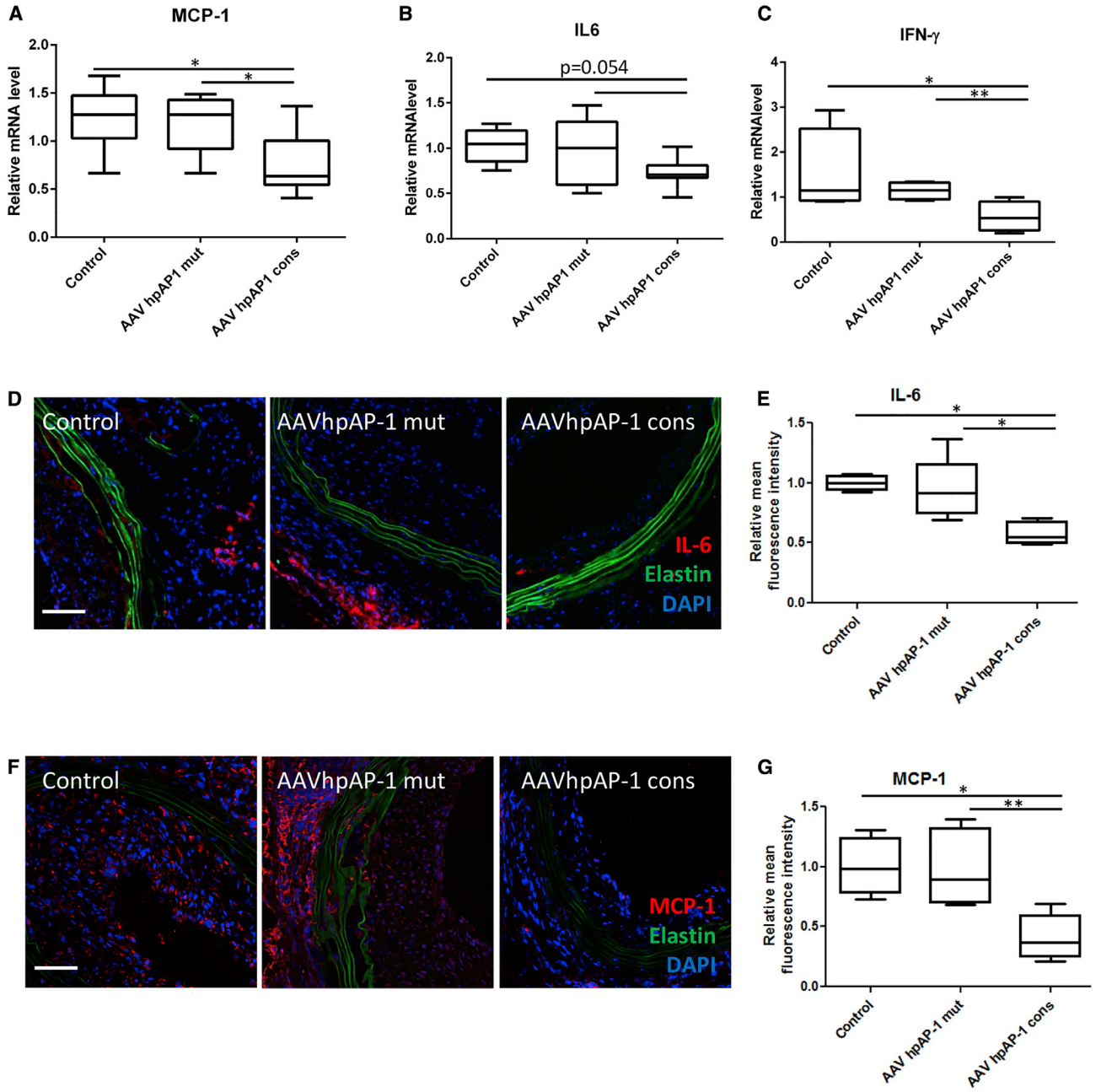



**Figure 6. Decreased Pro-inflammatory Markers in Aortic Grafts Transduced with AAV9SLR-Expressing hpAP-1 cons dONs.**

(A–C) Box-and-whisker plots of quantitative real-time PCR analysis of MCP-1 (A), IL-6 (B), and IFN-γ (C) in the depicted treatment groups. (D–G) Representative images showing IL-6 (D) and MCP-1 (F) protein levels after transduction and corresponding box-and-whisker plots of the relative fluorescence intensity (E and G). Nuclei were stained with DAPI (blue), and elastin autofluorescence was recorded in the green channel. Scale bar represents 25 μm. Horizontal bars in the boxes indicate median values, boxes indicate interquartile range, and whiskers indicate range of non-outlier values (*$p < 0.05$; *$p < 0.01$, n = 14 for control, n = 7 for AAV hpAP-1 mut, n = 9 for AAV hpAP-1 cons).

USA). The plots were generated by employing consensus and mutated dODNs in concentrations ranging from 0.1 pmol/L to 0.1 μmol/L. A nuclear extract isolated from 12-O-tetradecanoyl-phorbol-13-acetate (TPA)-stimulated K-562 cells was used as positive control for AP-1 transcriptional activation (Active Motif, Carlsbad, CA, USA). The graphs were achieved by plotting the logarithmic concentration of decoy ODNs against the absorbance, which was measured spectrophotometrically at 450 nm after performing the substrate reaction (Tecan, Crailsheim, Germany, USA).

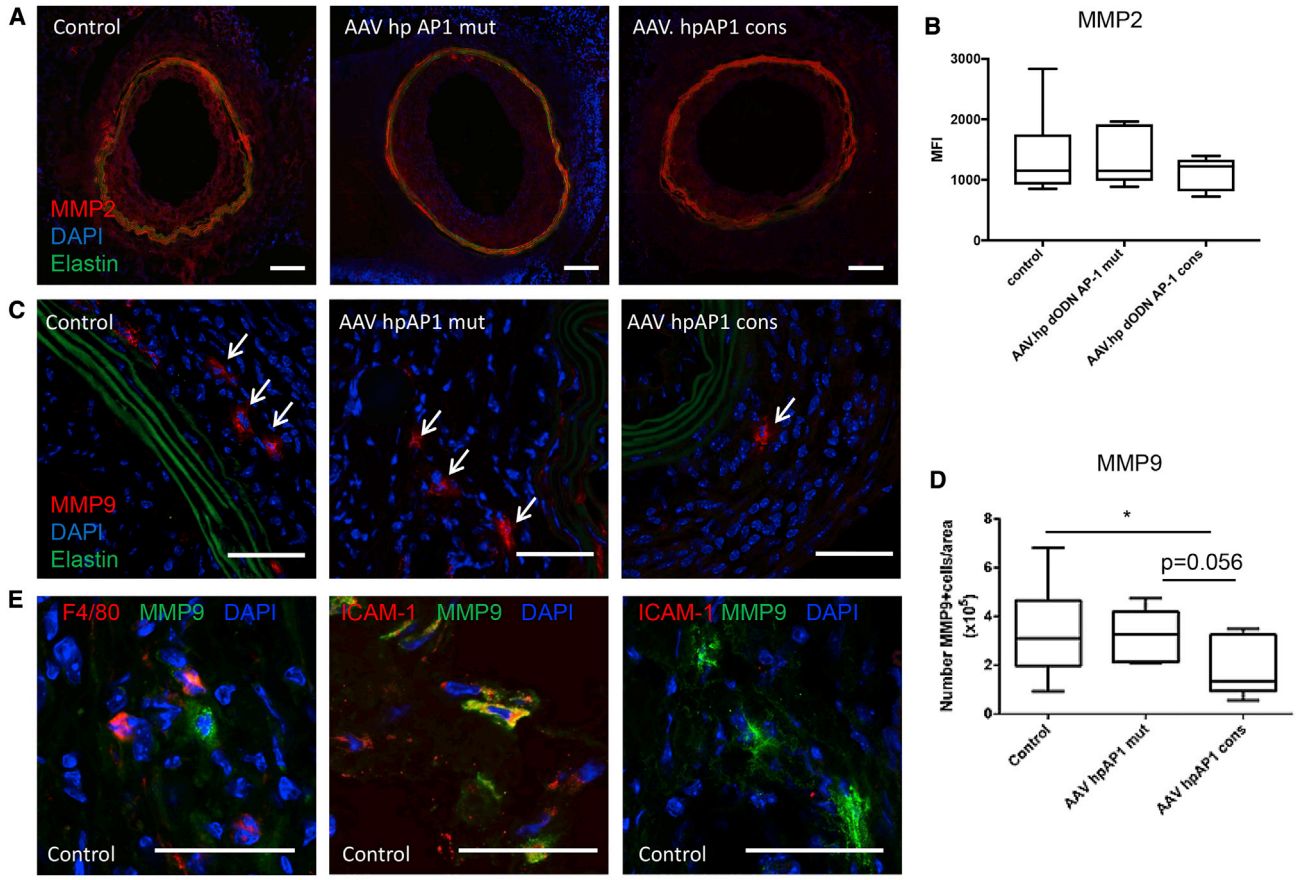



**Figure 7. Effect of AAV9SLR-Mediated of hpAP-1 cons dON Delivery on MMP Expression.**

(A) Representative MMP2 immunohistochemistry (red) images and (B) box-and-whisker plot showing the lack of effect of hpAP-1 consensus treatment. Elastin autofluorescence is pictured on the green channel, and DAPI (blue) marks cell nuclei. (C and D) Illustrative images (C) and box-and-whisker plot (D) of MMP9 immunostaining (red) in aortic cryosections. Single MMP9-positive cells, marked with arrows, were found mostly in the adventitia and media and infrequently in the neointima (*$p < 0.05$; $n = 7$ for AAV hpAP-1 mut, $n = 9$ for AAV hpAP-1 cons). Horizontal bars in the boxes indicate median values, boxes indicate interquartile range, and whiskers indicate range of non-outlier values. (E) Representative pictures demonstrating lack of colocalization of MMP9 signal (green) in the neointima of control grafts with the macrophage marker F4/80 (red, left image) and positive colocalization with ICAM-1-positive cells (red, center image). DAPI (blue) was used to label nuclei. Note that a small subset of MMP9-expressing cells as ICAM-1-positive immune cell population, while most of the MMP9 immunopositive cells were of different origin (right image). Scale bar represents 25 μm.

### Fluorescence *In Situ* Hybridization and Determination of Transduction Efficacy

Fluorescence *in situ* hybridization (FISH) was performed to detect the intracellularly formed hairpin AP-1 dON in the graft tissue according to standard protocols.[62] A molecular beacon (Biomers, Ulm, Germany) with complementary sequence to the hairpin AP-1 dODNs was used as a probe. In a hybridized state, the molecular beacon itself does not emit fluorescence signal due to the dye (5′-Cy5) and the quencher (3′-black hole quencher, BHQ) being located proximally. After hybridization to the target sequence, red fluorescence was recorded using confocal microscopy (LSM 800, Zeiss, Oberkochen, Germany). To quantify the percentage of hp AP-1 dON-transduced cells in the aortic tissue, four representative fields per section and two sections per graft were examined under × 20 magnification using a confocal microscope (LSM 800, Zeiss, Oberkochen, Germany). The number of AP-1 beacon-positive cells was divided by the number of DAPI-stained nuclei to determine the percent positive transduction. Approximately 1,000 cells were counted from each graft.

### Heterotropic Aortic Transplantation

All animal experiments were performed with permission of the local animal welfare committee (Regional Council Karlsruhe, Germany, permission number G100/14) and conform to the guidelines from Directive 2010/63/EU of the European Parliament on the protection of animals used for scientific purposes or the current NIH guidelines. Female DBA/2 (H-$2^d$) and C57BL/6J (H-$2^b$) mice[16] ages of 6–12 weeks were used as donor and recipient mice, respectively. The animals were purchased from Janvier Labs, Germany, and housed in the interfaculty biomedical research facility (IBF), Heidelberg University, Germany.

Descending thoracic aortae of DBA/2 mice were transplanted into C57CL/6 mice in infrarenal position, as already described.[63] Donor

mice were euthanized with $CO_2$. Thoracic cavity was opened, left ventricle was punctured and the arterial circulatory system was perfused with 5 mL NaCl (4°C, 0.9%, Braun, Melsungen, Germany). Descending aorta was harvested and incubated for 30 min in NaCl (B. Braun, Melsungen, Germany) as control or 50 μL AAV9SLR solution ($10^{12}$ vector genomes [VG]/mL), respectively.

Recipient C57BL/6J mice were anesthetized by inhalation of 5% isoflurane. Novalgin (500 mg/mL novaminsulfon-ratiopharm, Germany; 200 mg/kg body weight) and Carprieve (50 mg/mL carprofen, Norbrook Laboratories, Northern Ireland; 5 mg/kg body weight) were injected intraperitoneally. The abdominal cavity of recipient mice was opened and the infrarenal aorta was dissected. Titanium clips were applied and the aorta was transected. Grafts were connected to recipient aorta with two end-to-end anastomoses (Prolene 11-0, nylon black, S&T, Neuhausen, Switzerland). After removal of the clips the graft was re-perfused. Cyclosporine A (10 mg/kg body weight, Sandimmun, Novartis) and Temgesic (buprenorphin, 0.05 mg/kg body weight) for analgesia and CsA (10 mg/kg body weight, Sandimmun, Novartis) were injected intraperitoneally. Novalgin (500 mg/mL novaminsulfon-ratiopharm, Germany; 200 mg/kg body weight) and Carprieve (50 mg/mL carprofen, Norbrook Laboratories, Northern Ireland; 5 mg/kg body weight) were injected every 8 h within the first 3 postoperative days. CsA was injected once daily for 30 days; afterward, mice were sacrificed and aortic tissues were explanted.

### Morphometric Analysis

7-μm thick frozen aortic sections (Microtom, HM 500 O, Walldorf, Germany) were randomly chosen from various intervals throughout the transplanted grafts and further stained with H&E according to standard protocols. Afterward, ImageJ (Fiji version 1.51p, NIH, USA) was used to measure neointimal and medial areas with two investigators blinded toward the treatment regimen. The ratio of the two analyzed parameters was used as a measure of lumen obstruction.

### Immunohistochemistry

Subsequent to fixation with paraformaldehyde (PFA) 4%, 5-μm-thick aortic sections were incubated with BSA 2.5% and further with antibodies recognizing the markers of interest: α-SMA, MCP-1, MMP2, MMP9, IL-6, VCAM-1, Sca-1, c-Jun (phospho S63) [Y172] (Abcam, Cambridge, UK), cyclin D2 (Biozol, Eching, Germany), ICAM-1 (Santa Cruz, Heidelberg, Germany), F4/80 (Dianova, Hamburg, Germany), and JNK (Invitrogen, Carlsbad, CA, USA). After a series of washing with PBS, incubation with corresponding secondary antibodies (Dianova, Hamburg, Germany) was performed, followed by counterstaining with nuclear DAPI. Fluorescent signals were detected using confocal microscopy (LSM 800, Zeiss, Oberkochen, Germany) and quantified using ImageJ. Four random regions per section and two sections per graft were analyzed.

### qRT-PCR

Total RNA was extracted from isolated aortic grafts using RNeasy mini kit (QIAGEN, Hilden, Germany) according to manufacturer's instructions. First-strand cDNA synthesis was performed employing Omniscript reverse transcriptase kit (QIAGEN) and OligodT primers (Promega, Mannheim, Germany). qPCR was carried out on a standard SYBR Green (QIAGEN, Hilden, Germany)-based protocol using specific primers for the genes of interest, as follows: MCP-1 forward, 5′-TTCCTCCACCACCATGCAG-3′; MCP-1 reverse, 5′-CCAGCC GGCAACTGTGA-3′; IL-6 forward, 5′-CCTCTGGTCTTCTGGA GTACC-3′; IL-6 reverse, 5′-ACTCCTTCTGTGACTCCAGC-3′; RPL32 forward, 5′-GGGAGCAACAAGAAAACCAA-3′; RPL32 reverse 5′-ATTGTGGACCAGGAACTTGC-3′.

### Data Analysis

Data are shown as mean ± SD. GraphPad Prism 7 software was used to assess statistical significance between the groups, and one-way ANOVA analysis was employed to compare the different treatment groups. The Shapiro-Wilk test was used to prove that the results have a normal distribution. Tukey's multiple-comparison test was employed as a post hoc test to compare difference between single groups. A p value lower than 0.05 was considered statistically significant.

## SUPPLEMENTAL INFORMATION

Supplemental Information can be found online at https://doi.org/10.1016/j.omtm.2019.09.009.

## AUTHOR CONTRIBUTIONS

A.R. participated in experimental procedures, in evaluation of the data, and in the writing of the manuscript. M.F. participated in performing animal surgeries and experimental procedures and in evaluation of the data. F.M. and A.W. participated in experimental procedures. K.R. participated in histological evaluation of the data. A.J. was responsible for the virus production. M.K., M.H., K.K., and O.J.M. contributed to the design of the study and provided administrative and supervisory support. R.A. participated in the design of the experimental procedures and in performing animal surgeries. A.H.W. planned and supervised the study and wrote the manuscript.

## CONFLICTS OF INTEREST

The authors declare no competing interests.

## ACKNOWLEDGMENTS

This work was supported by the Dietmar Hopp Foundation, St. Leon-Rot, Germany (project no. 23011198).

## REFERENCES

1. Patel, J.K., Kittleson, M., and Kobashigawa, J.A. (2011). Cardiac allograft rejection. Surgeon *9*, 160–167.
2. Autieri, M.V. (2003). Allograft-induced proliferation of vascular smooth muscle cells: potential targets for treating transplant vasculopathy. Curr. Vasc. Pharmacol. *1*, 1–9.
3. Mitchell, R.N., and Libby, P. (2007). Vascular remodeling in transplant vasculopathy. Circ. Res. *100*, 967–978.
4. Chih, S., Chong, A.Y., Mielniczuk, L.M., Bhatt, D.L., and Beanlands, R.S. (2016). Allograft Vasculopathy: The Achilles' Heel of Heart Transplantation. J. Am. Coll. Cardiol. *68*, 80–91.
5. Orr, A.W., Hastings, N.E., Blackman, B.R., and Wamhoff, B.R. (2010). Complex regulation and function of the inflammatory smooth muscle cell phenotype in atherosclerosis. J. Vasc. Res. *47*, 168–180.

6. Viedt, C., Vogel, J., Athanasiou, T., Shen, W., Orth, S.R., Kübler, W., and Kreuzer, J. (2002). Monocyte chemoattractant protein-1 induces proliferation and interleukin-6 production in human smooth muscle cells by differential activation of nuclear factor-kappaB and activator protein-1. Arterioscler. Thromb. Vasc. Biol. *22*, 914–920.

7. Rao, G.N., Katki, K.A., Madamanchi, N.R., Wu, Y., and Birrer, M.J. (1999). JunB forms the majority of the AP-1 complex and is a target for redox regulation by receptor tyrosine kinase and G protein-coupled receptor agonists in smooth muscle cells. J. Biol. Chem. *274*, 6003–6010.

8. Xie, S., Nie, R., Wang, J., Li, F., and Yuan, W. (2009). Transcription factor decoys for activator protein-1 (AP-1) inhibit oxidative stress-induced proliferation and matrix metalloproteinases in rat cardiac fibroblasts. Transl. Res. *153*, 17–23.

9. Angel, P., and Karin, M. (1991). The role of Jun, Fos and the AP-1 complex in cell-proliferation and transformation. Biochim. Biophys. Acta *1072*, 129–157.

10. Roebuck, K.A., and Finnegan, A. (1999). Regulation of intercellular adhesion molecule-1 (CD54) gene expression. J. Leukoc. Biol. *66*, 876–888.

11. Schonthaler, H.B., Guinea-Viniegra, J., and Wagner, E.F. (2011). Targeting inflammation by modulating the Jun/AP-1 pathway. Ann. Rheum. Dis. *70* (*Suppl 1*), i109–i112.

12. Sirum-Connolly, K., and Brinckerhoff, C.E. (1991). Interleukin-1 or phorbol induction of the stromelysin promoter requires an element that cooperates with AP-1. Nucleic Acids Res. *19*, 335–341.

13. Buchwald, A.B., Wagner, A.H., Webel, C., and Hecker, M. (2002). Decoy oligodeoxynucleotide against activator protein-1 reduces neointimal proliferation after coronary angioplasty in hypercholesterolemic minipigs. J. Am. Coll. Cardiol. *39*, 732–738.

14. Hölschermann, H., Stadlbauer, T.H., Wagner, A.H., Fingerhuth, H., Muth, H., Rong, S., Güler, F., Tillmanns, H., and Hecker, M. (2006). STAT-1 and AP-1 decoy oligonucleotide therapy delays acute rejection and prolongs cardiac allograft survival. Cardiovasc. Res. *71*, 527–536.

15. Stadlbauer, T.H., Wagner, A.H., Hölschermann, H., Fiedel, S., Fingerhuth, H., Tillmanns, H., Bohle, R.M., and Hecker, M. (2008). AP-1 and STAT-1 decoy oligodeoxynucleotides attenuate transplant vasculopathy in rat cardiac allografts. Cardiovasc. Res. *79*, 698–705.

16. Bickerstaff, A.A., Wang, J.J., Pelletier, R.P., and Orosz, C.G. (2001). Murine renal allografts: spontaneous acceptance is associated with regulated T cell-mediated immunity. J. Immunol. *167*, 4821–4827.

17. Onuta, G., van Ark, J., Rienstra, H., Boer, M.W., Klatter, F.A., Bruggeman, C.A., Zeebregts, C.J., Rozing, J., and Hillebrands, J.L. (2010). Development of transplant vasculopathy in aortic allografts correlates with neointimal smooth muscle cell proliferative capacity and fibrocyte frequency. Atherosclerosis *209*, 393–402.

18. Spira, D., Grözinger, G., Domschke, N., Bantleon, R., Schmehl, J., Wiskirchen, J., and Wiesinger, B. (2015). Cell Cycle Regulation of Smooth Muscle Cells–Searching for Inhibitors of Neointima Formation: Is Combretastatin A4 an Alternative to Sirolimus and Paclitaxel? J. Vasc. Interv. Radiol. *26*, 1388–1395.

19. Valantine, H.A. (2003). Cardiac allograft vasculopathy: central role of endothelial injury leading to transplant "atheroma". Transplantation *76*, 891–899.

20. Hanidziar, D., and Koulmanda, M. (2010). Inflammation and the balance of Treg and Th17 cells in transplant rejection and tolerance. Curr. Opin. Organ Transplant. *15*, 411–415.

21. Liang, Y., Christopher, K., Finn, P.W., Colson, Y.L., and Perkins, D.L. (2007). Graft produced interleukin-6 functions as a danger signal and promotes rejection after transplantation. Transplantation *84*, 771–777.

22. van Buul, J.D., Kanters, E., and Hordijk, P.L. (2007). Endothelial signaling by Ig-like cell adhesion molecules. Arterioscler. Thromb. Vasc. Biol. *27*, 1870–1876.

23. Ardehali, A., Laks, H., Drinkwater, D.C., Ziv, E., and Drake, T.A. (1995). Vascular cell adhesion molecule-1 is induced on vascular endothelia and medial smooth muscle cells in experimental cardiac allograft vasculopathy. Circulation *92*, 450–456.

24. Tanaka, H., Sukhova, G.K., Swanson, S.J., Cybulsky, M.I., Schoen, F.J., and Libby, P. (1994). Endothelial and smooth muscle cells express leukocyte adhesion molecules heterogeneously during acute rejection of rabbit cardiac allografts. Am. J. Pathol. *144*, 938–951.

25. Alraies, M.C., and Eckman, P. (2014). Adult heart transplant: indications and outcomes. J. Thorac. Dis. *6*, 1120–1128.

26. Stehlik, J., Edwards, L.B., Kucheryavaya, A.Y., Benden, C., Christie, J.D., Dobbels, F., Kirk, R., Rahmel, A.O., and Hertz, M.I. (2011). The Registry of the International Society for Heart and Lung Transplantation: Twenty-eighth Adult Heart Transplant Report–2011. J. Heart Lung Transplant. *30*, 1078–1094.

27. Schmauss, D., and Weis, M. (2008). Cardiac allograft vasculopathy: recent developments. Circulation *117*, 2131–2141.

28. Stubbendorff, M., Deuse, T., Hammel, A., Robbins, R.C., Reichenspurner, H., and Schrepfer, S. (2010). Orthotopic aortic transplantation: a rat model to study the development of chronic vasculopathy. J. Vis. Exp. *2010*, 1989.

29. Lyon, A.R., Sato, M., Hajjar, R.J., Samulski, R.J., and Harding, S.E. (2008). Gene therapy: targeting the myocardium. Heart *94*, 89–99.

30. Zuckerbraun, B.S., and Tzeng, E. (2002). Vascular gene therapy: a reality of the 21st century. Arch. Surg. *137*, 854–861.

31. Varadi, K., Michelfelder, S., Korff, T., Hecker, M., Trepel, M., Katus, H.A., Kleinschmidt, J.A., and Müller, O.J. (2012). Novel random peptide libraries displayed on AAV serotype 9 for selection of endothelial cell-directed gene transfer vectors. Gene Ther. *19*, 800–809.

32. Xiao, X., Gang, Y., Wang, H., Wang, J., Zhao, L., Xu, L., and Liu, Z. (2015). Double-stranded RNA transcribed from vector-based oligodeoxynucleotide acts as transcription factor decoy. Biochem. Biophys. Res. Commun. *457*, 221–226.

33. Burger, K., and Gullerova, M. (2015). Swiss army knives: non-canonical functions of nuclear Drosha and Dicer. Nat. Rev. Mol. Cell Biol. *16*, 417–430.

34. Ahn, J.D., Morishita, R., Kaneda, Y., Lee, S.J., Kwon, K.Y., Choi, S.Y., Lee, K.U., Park, J.Y., Moon, I.J., Park, J.G., et al. (2002). Inhibitory effects of novel AP-1 decoy oligodeoxynucleotides on vascular smooth muscle cell proliferation in vitro and neointimal formation in vivo. Circ. Res. *90*, 1325–1332.

35. Arif, R., Franz, M., Remes, A., Zaradzki, M., Hecker, M., Karck, M., Müller, O.J., Kallenbach, K., and Wagner, A.H. (2019). Reduction of Transplant Vasculopathy by Intraoperative Nucleic Acid-based Therapy in a Mouse Aortic Allograft Model. Thorac. Cardiovasc. Surg. *67*, 503–512.

36. Ahn, J.D., Morishita, R., Kaneda, Y., Kim, H.J., Kim, Y.D., Lee, H.J., Lee, K.U., Park, J.Y., Kim, Y.H., Park, K.K., et al. (2004). Transcription factor decoy for AP-1 reduces mesangial cell proliferation and extracellular matrix production in vitro and in vivo. Gene Ther. *11*, 916–923.

37. Jun, D.Y., Kim, M.K., Kim, I.G., and Kim, Y.H. (1997). Characterization of the murine cyclin D2 gene: exon/intron organization and promoter activity. Mol. Cells *7*, 537–543.

38. Arif, R., Zaradzki, M., Remes, A., Seppelt, P., Kunze, R., Schröder, H., Schwill, S., Ensminger, S.M., Robinson, P.N., Karck, M., et al. (2017). AP-1 Oligodeoxynucleotides Reduce Aortic Elastolysis in a Murine Model of Marfan Syndrome. Mol. Ther. Nucleic Acids *9*, 69–79.

39. Pober, J.S., Jane-wit, D., Qin, L., and Tellides, G. (2014). Interacting mechanisms in the pathogenesis of cardiac allograft vasculopathy. Arterioscler. Thromb. Vasc. Biol. *34*, 1609–1614.

40. Wyburn, K.R., Jose, M.D., Wu, H., Atkins, R.C., and Chadban, S.J. (2005). The role of macrophages in allograft rejection. Transplantation *80*, 1641–1647.

41. Lee, I., Wang, L., Wells, A.D., Ye, Q., Han, R., Dorf, M.E., Kuziel, W.A., Rollins, B.J., Chen, L., and Hancock, W.W. (2003). Blocking the monocyte chemoattractant protein-1/CCR2 chemokine pathway induces permanent survival of islet allografts through a programmed death-1 ligand-1-dependent mechanism. J. Immunol. *171*, 6929–6935.

42. Yang, J., Reutzel-Selke, A., Steier, C., Jurisch, A., Tullius, S.G., Sawitzki, B., Kolls, J., Volk, H.D., and Ritter, T. (2003). Targeting of macrophage activity by adenovirus-mediated intragraft overexpression of TNFRp55-Ig, IL-12p40, and vIL-10 ameliorates adenovirus-mediated chronic graft injury, whereas stimulation of macrophages by overexpression of IFN-gamma accelerates chronic graft injury in a rat renal allograft model. J. Am. Soc. Nephrol. *14*, 214–225.

43. Ahmad, M., Theofanidis, P., and Medford, R.M. (1998). Role of activating protein-1 in the regulation of the vascular cell adhesion molecule-1 gene expression by tumor necrosis factor-alpha. J. Biol. Chem. *273*, 4616–4621.

44. Hansson, G.K., and Libby, P. (2006). The immune response in atherosclerosis: a double-edged sword. Nat. Rev. Immunol. *6*, 508–519.

45. Wang, N., Verna, L., Liao, Hl, Ballard, A., Zhu, Y., and Stemerman, M.B. (2001). Adenovirus-mediated overexpression of dominant-negative mutant of c-Jun prevents intercellular adhesion molecule-1 induction by LDL: a critical role for activator protein-1 in endothelial activation. Arterioscler. Thromb. Vasc. Biol. *21*, 1414–1420.

46. Berceli, S.A., Jiang, Z., Klingman, N.V., Pfahnl, C.L., Abouhamze, Z.S., Frase, C.D., Schultz, G.S., and Ozaki, C.K. (2004). Differential expression and activity of matrix metalloproteinases during flow-modulated vein graft remodeling. J. Vasc. Surg. *39*, 1084–1090.

47. Hasegawa, H., Senga, T., Ito, S., Iwamoto, T., and Hamaguchi, M. (2009). A role for AP-1 in matrix metalloproteinase production and invadopodia formation of v-Crk-transformed cells. Exp. Cell Res. *315*, 1384–1392.

48. Wang, W.M., Wu, S.Y., Lee, A.Y., and Chiang, C.M. (2011). Binding site specificity and factor redundancy in activator protein-1-driven human papillomavirus chromatin-dependent transcription. J. Biol. Chem. *286*, 40974–40986.

49. Mason, D.P., Kenagy, R.D., Hasenstab, D., Bowen-Pope, D.F., Seifert, R.A., Coats, S., Hawkins, S.M., and Clowes, A.W. (1999). Matrix metalloproteinase-9 overexpression enhances vascular smooth muscle cell migration and alters remodeling in the injured rat carotid artery. Circ. Res. *85*, 1179–1185.

50. Johnson, J.L., Dwivedi, A., Somerville, M., George, S.J., and Newby, A.C. (2011). Matrix metalloproteinase (MMP)-3 activates MMP-9 mediated vascular smooth muscle cell migration and neointima formation in mice. Arterioscler. Thromb. Vasc. Biol. *31*, e35–e44.

51. Braun, M., Pietsch, P., Schrör, K., Baumann, G., and Felix, S.B. (1999). Cellular adhesion molecules on vascular smooth muscle cells. Cardiovasc. Res. *41*, 395–401.

52. Lawson, C., Ainsworth, M.E., McCormack, A.M., Yacoub, M., and Rose, M.L. (2001). Effects of cross-linking ICAM-1 on the surface of human vascular smooth muscle cells: induction of VCAM-1 but no proliferation. Cardiovasc. Res. *50*, 547–555.

53. Hareendran, S., Balakrishnan, B., Sen, D., Kumar, S., Srivastava, A., and Jayandharan, G.R. (2013). Adeno-associated virus (AAV) vectors in gene therapy: immune challenges and strategies to circumvent them. Rev. Med. Virol. *23*, 399–413.

54. Tse, L.V., Moller-Tank, S., and Asokan, A. (2015). Strategies to circumvent humoral immunity to adeno-associated viral vectors. Expert Opin. Biol. Ther. *15*, 845–855.

55. García Sáez, D., Zych, B., Sabashnikov, A., Bowles, C.T., De Robertis, F., Mohite, P.N., Popov, A.F., Maunz, O., Patil, N.P., Weymann, A., et al. (2014). Evaluation of the organ care system in heart transplantation with an adverse donor/recipient profile. Ann. Thorac. Surg. *98*, 2099–2105, discussion 2105–2106.

56. Messer, S., Ardehali, A., and Tsui, S. (2015). Normothermic donor heart perfusion: current clinical experience and the future. Transpl. Int. *28*, 634–642.

57. Hecker, M., and Wagner, A.H. (2017). Transcription factor decoy technology: A therapeutic update. Biochem. Pharmacol. *144*, 29–34.

58. Schinkel, S., Bauer, R., Bekeredjian, R., Stucka, R., Rutschow, D., Lochmüller, H., Kleinschmidt, J.A., Katus, H.A., and Müller, O.J. (2012). Long-term preservation of cardiac structure and function after adeno-associated virus serotype 9-mediated microdystrophin gene transfer in mdx mice. Hum. Gene Ther. *23*, 566–575.

59. Ying, Y., Müller, O.J., Goehringer, C., Leuchs, B., Trepel, M., Katus, H.A., and Kleinschmidt, J.A. (2010). Heart-targeted adeno-associated viral vectors selected by in vivo biopanning of a random viral display peptide library. Gene Ther. *17*, 980–990.

60. Grieger, J.C., Choi, V.W., and Samulski, R.J. (2006). Production and characterization of adeno-associated viral vectors. Nat. Protoc. *1*, 1412–1428.

61. Werfel, S., Jungmann, A., Lehmann, L., Ksienzyk, J., Bekeredjian, R., Kaya, Z., Leuchs, B., Nordheim, A., Backs, J., Engelhardt, S., et al. (2014). Rapid and highly efficient inducible cardiac gene knockout in adult mice using AAV-mediated expression of Cre recombinase. Cardiovasc. Res. *104*, 15–23.

62. Peng, X.H., Cao, Z.H., Xia, J.T., Carlson, G.W., Lewis, M.M., Wood, W.C., and Yang, L. (2005). Real-time detection of gene expression in cancer cells using molecular beacon imaging: new strategies for cancer research. Cancer Res. *65*, 1909–1917.

63. Seppelt, P.C., Schwill, S., Weymann, A., Arif, R., Weber, A., Zaradzki, M., Richter, K., Ensminger, S., Robinson, P.N., Wagner, A.H., et al. (2016). Loss of Endothelial Barrier in Marfan Mice (mgR/mgR) Results in Severe Inflammation after Adenoviral Gene Therapy. PLoS ONE *11*, e0148012.